Available online at www.sciencedirect.com
SCIENCE DIRECT®
Polymer 44 (2003) 6387–6395
polymer
www.elsevier.com/locate/polymer

Synthesis and characterization of exfoliated poly(styrene-co-methyl methacrylate)/clay nanocomposites via emulsion polymerization with AMPS

Mingzhe Xu, Yeong Suk Choi, Yoon Kyung Kim, Ki Hyun Wang, In Jae Chung*

Department of Chemical and Biomolecular Engineering, Korea Advanced Institute of Science and Technology(KAIST), 373-1, Guseong-dong, Yuseong-gu, Daejeon 305-701, South Korea

Received 17 September 2002; received in revised form 16 April 2003; accepted 11 July 2003

Abstract

A method was described for synthesis of exfoliated poly(styrene-co-methyl methacrylate)/clay nanocomposites through an emulsion polymerization with reactive surfactant, 2-acrylamido-2-methyl-1-propane sulfonic (AMPS) which made the polymer end-tethered on pristine Na-MMT.

AMPS widened the gap between clay layers and facilitates comonomers penetrate into clay. Silicate layers affect the composition of comonomers, for example A0.3M10S10T5 showed the elevated composition of MMA end tethered on silicate when compared to the feed ratio and polar methyl methacrylate (MMA) was considered to have the stronger interaction with clay layers than styrene.

The exfoliated structure of extracted nanocomposite was confirmed by XRD and transmission electron microscopy. The onset of thermal decomposition for nanocomposites shifted to a higher temperature than that for neat copolymer. The dynamic moduli of nanocomposites increase with clay content. Dynamic storage modulus and complex viscosity increased as the clay content increased. In low frequency region all prepared nanocomposites exhibited apparent low-frequency plateaus in the linear storage modulus. Complex viscosity showed shear-thinning behavior as the clay content increases.

Keywords: Polystyrene/polymethylmethacrylate copolymer; Clay; Nanocomposite

1. Introduction

Polymer/silicate nanocomposite is a novel class of composite. At least one dimension of the dispersed particles of composite is in the nanometer range. Because of many advantages such as high mechanical property, good gas barrier, flame retardation and etc., polymer/clay nanocomposites have been intensely investigated [1–14]. Pioneering work of nylon–clay hybrid composites has been achieved by researchers at Toyota for light-weight material applications [15–17].

One can obtain two types of nanocomposites; Intercalated structures and exfoliated structures. Especially exfoliated polymer–clay hybrids offer the improved mechanical and thermal properties because the homogeneous dispersion of clay in polymer matrix, as well as large interfacial area of clay layers.

Pristine clay is naturally hydrophilic, and polymers are often hydrophobic [18–19]. The hydrophilic nature of pristine clay impedes its homogeneous dispersion in polymer matrix. So, the clay modified with alkylammonium facilitates its interaction with a polymer because the alkylammonium makes the hydrophilic clay surface organophilic. Most of researches on synthesis of nanocomposites are focused on the organical modification of layered silicates (OLS) [20–29]. Many researchers have reported fabrication of polystyrene (PS)/clay nanocomposites [30–44] and polymethylmethacrylate (PMMA)/clay nanocomposites because of their big market volume [45–54], but most PS and PMMA/clay nanocomposites show the intercalated form of clay.

Our very recent article on the fabrication of PMMA/clay nanocomposite has confirmed that a simple and convenient technique of emulsion polymerization can offer an effective

* Corresponding author. Tel.: +82-42-869-3916; fax: +82-42-869-3910.
E-mail address: chung@kaist.ac.kr (I.J. Chung).

0032-3861/$ - see front matter © 2003 Elsevier Ltd. All rights reserved.
doi:10.1016/S0032-3861(03)00653-0

and potential approach for the exfoliated polymer/clay nanocomposites with a reactive surfactant, AMPS, by using untreated pristine Na-MMT [55]. The important advantage of emulsion polymerization is employment of water as a dispersion medium. Water makes the galleries of layered silicates widen without any chemical treatment. A reactive surfactant, 2-acrylamido-2-methyl-1-propane sulfonic (AMPS) [56–58], has amido and sulfonic acid groups in the molecule. Therefore polymers with AMPS may be tethered on silicate layers due to the strong interaction of amido group with pristine silicates. Sulfonic acid acts as a surface-active material.

MMA can make H-bond or van-der Waals attraction with OH, SiO, Al–O presented in silicate sheet. It is believed that MMA would polymerize within and near silicate layers. This mechanism may contribute to the exfoliation of nanocomposites. Poly(styrene-co-methyl methacrylate) [P(S-co-MMA)] may be in the middle of hydrophobic–hydrophilic balance.

Here, we fixed the ratio of comonomer as 1:1 (MMA/styrene) by weight and varied silicate contents. We will observe the morphology of nanocomposites in this polymerization system. This may give more helpful information to understand exfoliation behavior of clay layers that occurs that occurring in copolymerization system such as SBR latex.

The P(S-co-MMA)/Na-MMT nanocomposites will be synthesized and characterized by a simple and convenient emulsion polymerization with a reactive surfactant AMPS. Their mechanical, thermal, and rheological properties are also investigated.

2. Experimental

2.1. Materials

Pristine Sodium montmorillonite (Na-MMT) was used as purchased from Kunimine Co. and it had a cation exchange capacity (CEC) of 119 mequiv./100 g.

MMA, styrene, AMPS and dodecylbenzenesulfonic acid sodium salt (DBS-Na) were purchased from Aldrich and used without further purification. Pristine Na-MMT was dispersed in deionized water for 24 h at ambient temperature before polymerization. Potassium persulate (KPS) of Junsei, an initiator, was recrystallized using deionized water. Tetrahydrofuran (THF), HPLC solvent grade, was purchased from Fluka for polymer recovery in extraction and the reverse ion exchange procedure. *n*-hexane, a non-solvent for P(S-co-MMA), was distilled at normal pressure. Lithium chloride (Junsei) was recrystallized with THF.

2.2. Preparation of P(S-co-MMA)/Na-MMT nanocomposites

Polymerization was carried out in two stages:

(1) Pristine Na-MMT dispersed in deionized water (from 0 to 5 wt% of Na-MMT relative to weight of comonomer), 5 g of comonomer (styrene and MMA), 0.3 g of AMPS, and deionized water were stirred at room temperature in a 1 L four-necked round bottom flask. The flask was equipped with a baffle stirrer, a reflux condenser, a nitrogen inlet, and a rubber septum. Twenty grams of initiator solution (KPS/water ratio = 1 g:99 g) was injected into the flask through a rubber septum by using a glass syringe. The mixture was stirred at 200 rpm for 1 h under nitrogen atmosphere at room temperature. Successively, the temperature was kept at 65 °C for 1 h. Then 5 g of DBS-Na aqueous solution was added to stabilize the particle in order to obtain a high conversion of polymerization. After adding DBS-Na we control reaction process directly to second stage.

(2) After the initial polymerization was completed, 15 g of comonomer was fed at the rate of 0.16 cm^3/min into the flask through a septum by using a syringe pump. After monomer feeding was completed, additional 5 g of KPS was added. Continuously the mixture was stirred for additional 4 h for polymerization after temperature was raised up to 85 °C. The sample was recovered from the flask and dried with a freeze-drying equipment for 6 days and further dried in a high vacuum oven at 80 °C for 3 days.

Before X-ray measurements a small amount of nanocomposites was extracted with THF in a Soxhlet extractor for 12 h to remove oligomers, water molecules, or surfactants. The extracted polymer/Na-MMT nanocomposite was dried under a highly reduced pressure at 100 °C for 50 h and molded to disc type at nominal 3000 psi of pressure. The basal space of clay layers was calculated from X-ray patterns.

2.3. Polymer recovery

Polymers in the nanocomposites were totally recovered by reverse ion exchange procedure described in the following way: 1 g of prepared nanocomposite, 0.3 g of LiCl and 80 ml of THF were stirred in a 250 ml flask at ambient temperature for 5 days [7]. The mixture was centrifuged at 6000 rpm for 30 min to separate polymers from the silicate cakes. After separating the clay by centrifugation, the polymer was recovered by precipitating in *n*-hexane with 0.45 μm membrane filter.

A small amount of nanocomposites was extracted with THF in a Soxhlet extractor for 12 h to remove molecules and polymer unbounded on clay layers. While the molecules bounded on silicates were obtained by the reverse ion exchange, after unbound polymers were segregated from nanocomposites by Soxhlet extraction for 5 days. Molecular weight of these molecules were measured by Tandem MS.

2.4. Characterization

Fourier transform infrared spectroscopy (FT-IR) was

performed on a infrared spectrometer (Bomem 102 model) at 4 cm^{-1} resolution. Infrared spectrum on KBr pellets was averaged over 20 scans on a FT-IR spectrometer. ^1H NMR spectrum was collected using a Bruker DMX 600 spectrometer employing THF as the solvent. Wide-angle X-ray diffraction (WAXD) analysis was performed on a Rigaku X-ray generator (Cu Kα radiation with $\lambda = 0.15406$ nm), at room temperature. A sample was prepared in the pellet form. The diffractograms were scanned at the rate of 2°/min in 2θ range of 1.2–10°. Molecular weight analysis was performed at room temperature by gel permeation chromatography (GPC). Water GPC system equipped with six styragel HR columns (two 500, two 10^3, 10^4, and 10^5) and Water 410 RID detector was used with the flow rate of THF 2 ml/min after calibration with 10 PMMA standards. Molecular weights of the molecules tethered on silicates after the reverse ion exchange with Li^+ were measured by Tandem MS, JMS HX-110/110A from JEOL Col. with FAB + (fast atom bombardment) ion mode, using nitrobenzyl alcohol as a matrix at 0.6 °C. Thermogravimetric analysis (TGA) was performed on a thermogravimetric analyzer (TA instruments) with a Perkin–Elmer thermobalance over the temperature range 25–600 °C at a rate of 10 °C/min under nitrogen atmosphere. The microstructure of nanocomposite was imaged using a transmission electron microscopy (TEM), Phillips CM-20. Acceleration voltage of TEM was 160 kV. The nanocomposite was sectioned into ultrathin slices (< 100 nm) using microtome equipped with a diamond knife at room temperature. Dynamic mechanical properties of nanocomposites were measured using a Rheometric Scientific DMTA4 with extensional mode. Dynamic moduli and tan δ of all samples were measured at the scan rate of 4 °C/min from 30 to 180 °C under 0.01% deformation at a frequency of 1 Hz. The bar type specimens were molded at 175 °C with dimensions $40 \times 10 \times 0.75$ mm^3 thick using a hot press.

Rheology measurements of nanocomposites were performed on an advanced rheometric expansion system in oscillatory mode with a parallel plate geometry using 25 mm diameter plates at 200 °C. Samples for melt rheology were molded in a disk shape by compression. Typical sample thickness had the range from 1.0 to 1.2 mm. All the experiments were performed under nitrogen atmosphere to minimize oxidative degradation of specimens.

3. Results and discussion

3.1. Preparation of P(S-co-MMA)/clay nanocomposites

The nanocomposite was marked by the letters M, S and T followed by a number. The letters M, S, and T denote MMA, styrene, and clay, respectively. The number followed by M and S stand for the weights of the monomer used in emulsion polymerization and the number following after T stands for weight percent of clay relative to monomers. For example, A0.3M10S10T3 nanocomposite includes 0.3 g of AMPS, 10 g of MMA, 10 g of styrene, 3 wt% Na-MMT relative to 20 g of comonomer (MMA and styrene).

The average molecular masses and polydispersities of P(S-co-MMA) obtained by the extraction of nanocomposite with THF are listed in Table 1. The M_w values of the copolymers are found to be in the order of 10^5 g/mol regardless the silicate content. It is believed that, molecular weight is not affected by the amount of clay in the range of conventional surfactant content used in our system.

Fig. 1 shows the FT-IR spectra of Na-MMT, AMPS, neat copolymer, and A0.3M10S10T3. The peaks around 3630 and 1650 cm^{-1} correspond to OH stretchings of silicate layers. The sharp peak centered at 1043 cm^{-1} is associated with the Si–O stretching vibration of silicate layer, and peaks at about 600 and 410 cm^{-1} with the stretching of Al–O and bending of Si–O. The peaks at 1610 cm^{-1} (vinyl stretching), 1364 and 1241 cm^{-1} (S=O), NH bending 1543 cm^{-1} are related to AMPS. Absorption bands at 2949 (C–H stretching), 1732 (C=O stretching), 1136–1200 (C–O stretching), 3028, 3064 (aromatic C–H stretching), and 760 cm^{-1} (aromatic C–H bending) are the consequences of the PS-co-PMMA copolymer respectively.

3.2. XRD analysis of clay solutions and nanocomposite films

The pristine Na-MMT has an interlayer spacing of $d = 1.14$ nm with 2θ value 7.7°, which is obtained from the peak position (d_{001}-reflection) of WAXD traces by using Bragg equation: $2d_{001}\sin\theta = \lambda$

where d_{001} is the interplanar distance of (001) reflection plane, θ is the diffraction angle and λ is the wavelength.

The XRD patterns of pristine Na-MMT dispersed in various solution conditions are shown in Fig. 2(a) which depicts the initial state of A0.3M10S10T5. The peak of Na-MMT dispersed in water occurs at 5.7° corresponding to the

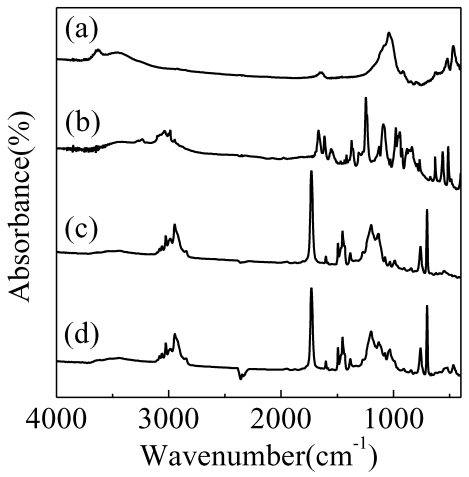

Fig. 1. FT-IR spectra of (a) pristine Na-MMT, (b) AMPS (reactive surfactant), (c) A0.3M10S10T0 (neat copolymer), (d) A0.3M10S10T3 nanocomposite (containing 3 wt% of Na-MMT).

Table 1
Molecular weights of polymeric materials recovered from P(S-co-MMA)/Na-MMT nanocomposites and neat copolymer and (MMA/Styrene) M/S ratio of molecules obtained by ^{1}H NMR

Sample code	$M_n \times 10^4$ (g/mol)	M_w (g/mol)	PDI (M_w/M_n)	Monomer composition tethered (M:S)[a]	Monomer feed ratio in moles (M:S)
A0.3M10S10T0	9.1	2.3×10^5	2.50		
A0.3M10S10T1	3.4	1.4×10^5	4.11		
A0.3M10S10T3	3.5	2.1×10^5	5.87	1.0:1.0	1.0:0.96
A0.3M10S10T5	5.2	2.8×10^5	5.34	1.0:0.49	1.0:0.96
A0.3M10S10T3R[b]		312			
A0.3M10S10T5R[b]		218			

R stand for the polymer recovered by the reverse ion exchange after the THF extraction, respectively.
[a] M and S stand for methyl methacrylate and styrene, respectively.
[b] Molecular weight obtained from Tandem MS analysis using FAB^+ ion method.

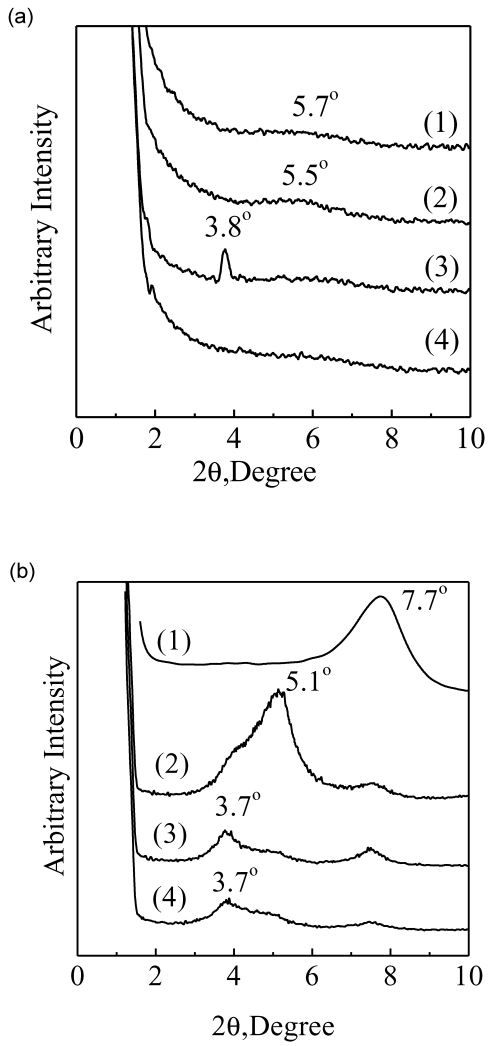

Fig. 2. X-ray diffraction patterns of (a) water dispersions of pristine Na-MMT under various conditions: (1) the dispersion of Na-MMT in water, (2) with comonomer, (3) with AMPS, and (4) with both AMPS and comonomer and (b) AMPS with different amount of clays after drying the water dispersions (1) pristine Na-MMT, (2) AMPS with 5 wt% (3) AMPS with 3 wt%, and (4) AMPS with 1 wt% of clay.

basal space of 1.55 nm in 2θ value, which means interlayer space of silicate is widened by water. The Na-MMT dispersed with comonomer in water shows the peak around 5.5° with the d_{001}-space of 1.61 nm. The Na-MMT dispersed with AMPS in water shows the peak around 3.8° with the space of 2.32 nm. The Na-MMT dispersion with AMPS and comonomer in water shows no peak. It indicate that AMPS intercalated in clay attracts comonomers to make the gap between clay layers widen.

The X-ray patterns for different contents of clay at fixed AMPS amount are shown in Fig. 2(b). The samples were freeze-dried for X-ray diffraction. The peaks for 1 and 3 wt% of clay appear at 3.74° with the basal space of 2.36 nm. The peak for 5 wt% of clay, at 5.13° with the basal space of 1.72 nm. The d_{001}-spacing for 1 and 3 wt% is wider than that for 5 wt%. It means that for a fixed amount of AMPS the amount of AMPS per clay for 1 and 3 wt% is lower than for 5 wt%.

Thermogravimetric analysis was used to determine the amount of AMPS inserted in the gallery of silicate. Various amounts of AMPS (100, 50 and 30% of CEC of the clay) were added to the mixture and stirred for additional 1 day. By centrifuging the mixtures at 8000 rpm for 30 min, clay with AMPS was segregated from the water. The clay cakes were freeze-dried for 7 days. The amount of AMPS loaded in clay is determined by the residual weight difference between clay with AMPS and the pristine clay at 600 °C in Fig. 3. The decomposition behavior of pure dried AMPS is inserted in the figure. The AMPS starts to decompose at about 185 °C and its residue at 600 °C is 7.6%. The weight loss below 105 °C results from adsorbed water. The residual weight percentage of pristine Na-MMT at 600 °C is 97.53%, and those of TA100, TA50 and TA30% are 90.40, 94.08, and 95.18%, respectively (T and A denote Na-MMT and AMPS, respectively. 100% means 100% of CEC of the clay). TA100% contains 147.3 mg of AMPS in 1 g of clay. TA50 and 30% have 110.5 and 99.5 mg of AMPS, respectively.

Fig. 4(a) shows a series of thin film XRD patterns obtained from pristine Na-MMT and nanocomposites which are not extracted by using a Soxhlet extraction apparatus

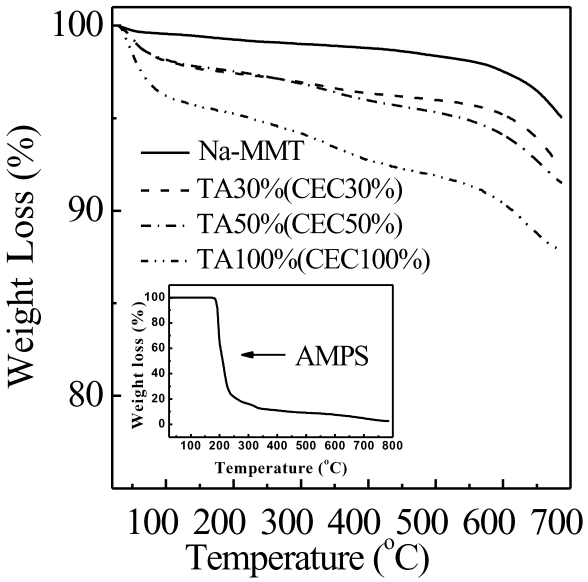

Fig. 3. Thermal gravimetric curves for Na-MMT with different amounts of AMPS and pristine Na-MMT under nitrogen atmosphere.

with THF. All nanocomposites show no peak and have the exfoliated structure.

Fig. 4(b) shows a series of thin film XRD patterns obtained from pristine Na-MMT and nanocomposites which are extracted by using a Soxhlet extraction apparatus with THF. A0.3M10S10T5 shows a peak at about 5.8° with the basal space of 1.52 nm, which indicates that the clays in the nanocomposite are intercalated still have the van-der Waals force interaction between layers.

In contrast, A0.3M10S10T1 and A0.3M10S10T3 show no peaks, indicating the exfoliation of clay up to 3 wt% of silicates.

3.3. Comonomer ratio inside clay layers by ^1H NMR spectrum

Fig. 5(a) represents ^{1}H NMR spectrum of copolymer obtained from A0.3M10S10T3 nanocomposite by the Soxhlet extraction with THF. Methoxy protons of MMA show peaks in the range of 2.1–3.8 δ. Methylene protons show peaks in the range of 1.1–2.1 δ. C–H protons of styrene show peaks in the range 2.1–2.6 δ. Phenyl group proton of styrene show peaks in the range of 6.2–7.5 δ. THF, a solvent of NMR, shows a peak at 3.58 and 1.73 δ. The peak at 2.48 δ corresponds to water peak. Aliphatic CH_3 proton of MMA show broad peaks in the range of 0.2–1.1 δ. These peaks are typical spectrum of random copolymer consisting of MMA and styrene. This spectrum is similar to those of other researchers who synthesized MMA/styrene copolymers [59]. The composition of MMA and styrene in copolymer extracted with THF shows the same ratio as in the feed, but the molecules tethered on silicate surface have a different composition.

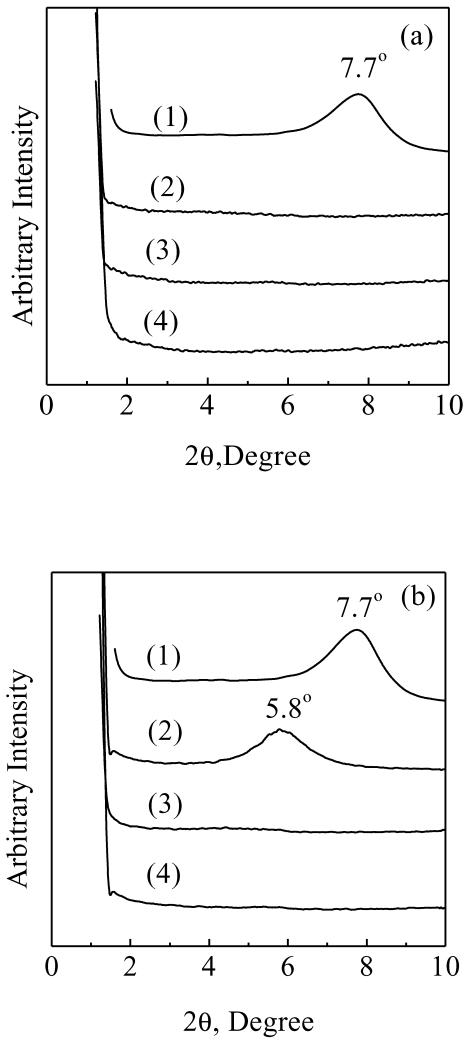

Fig. 4. X-ray diffraction patterns of (a) unextracted and (b) extracted A0.3M10S10T nanocomposites series by using THF: (1) pristine Na-MMT, (2) A0.3M10S10T5, (3) A0.3M10S10T3, (4) A0.3M10S10T1. Pristine Na-MMT measured by powder method was given as a reference.

Fig. 5(b) represents ^{1}H NMR spectrum of molecules tethered on clay in A0.3M10S10T3. These polymer molecules were obtained by the reverse ion exchange after the polymers were removed by a Soxhlet extraction with THF in Fig. 5(a). THF was used as a solvent without TMS. We also calculated the peak area ratio for MMA to styrene in a copolymer molecule in the range of 1.1–2.1 δ for methylene protons and in the range of 6.2–7.5 δ for phenyl group proton of styrene (Table 1).

The peak area ratio for MMA to styrene in A0.3M10S10T3 is about 1:1 and the ratio for A0.3M10S10T5 in Table 1 is about 1:0.49 though the ratio of MMA to styrene in the feed is about 1:0.96 in moles. MMA occupies a larger portion in the clay than styrene when the nanocomposite has high clay content. It is believed that MMA is more attractive to clay layers than styrene due to the polar group of MMA.

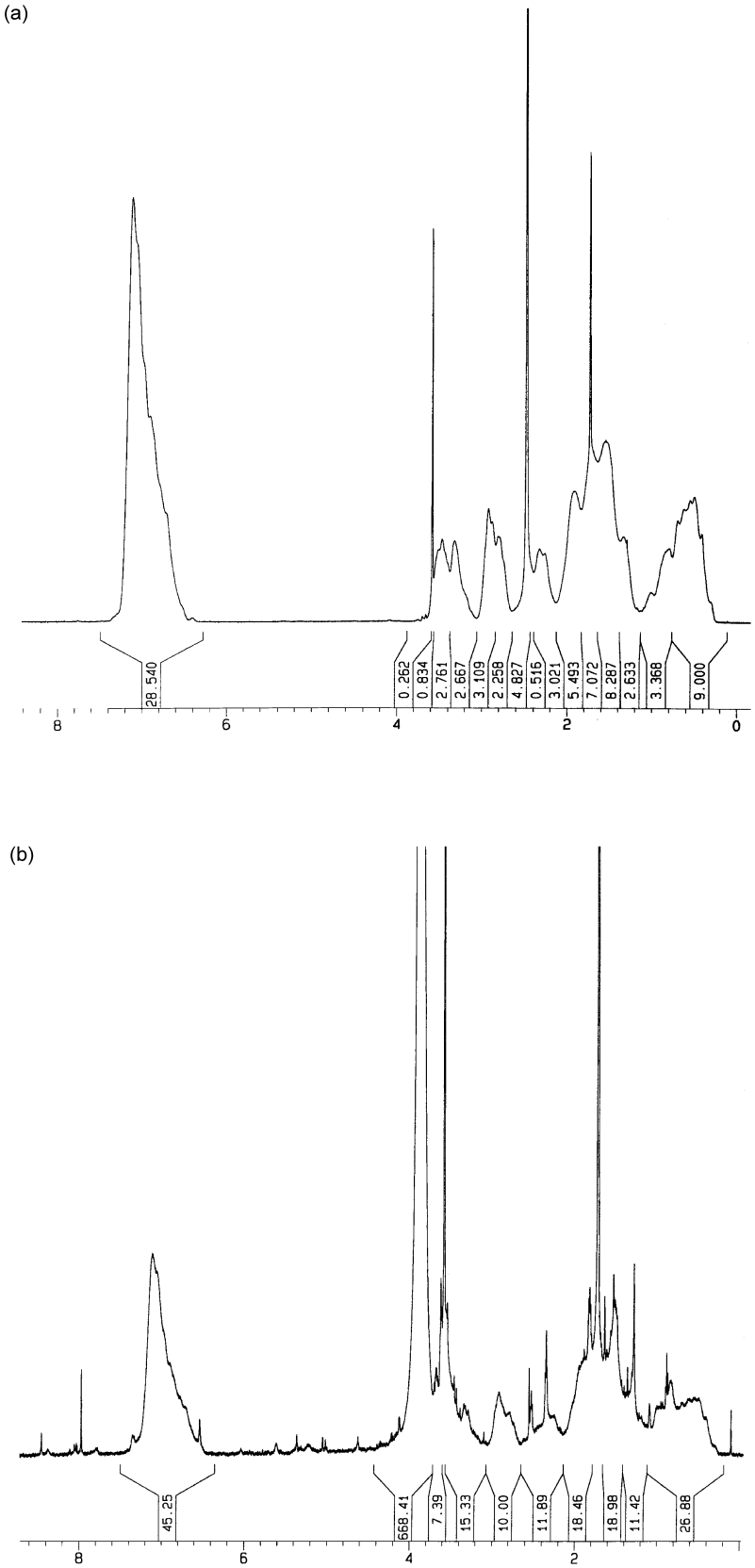

Fig. 5. ^{1}H NMR spectra of (a) polymer recovered from A0.3M10S10T3 by a Soxhlet extraction for 5 days, and (b) molecules tethered on A0.3M10S10T3 by the reverse ion exchange with THF/LiCl after THF extraction with Soxhlet extraction apparatus for 5 days.

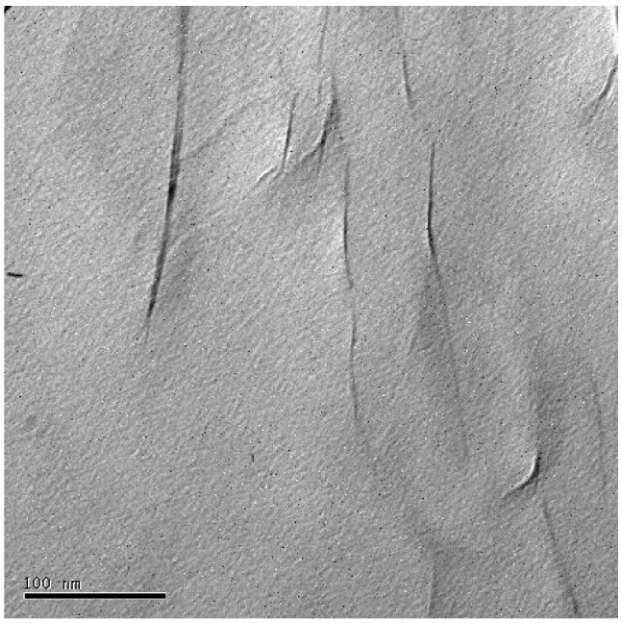

Fig. 6. Transmission electron microscopy (TEM) of extracted A0.3M10S10T3 nanocomposite.

3.4. TEM analysis of nanocomposites

The complete exfoliation of the silicate layers cannot be judged from only these diffractograms. TEM was adopted to confirm the morphology of extracted nanocomposite. Fig. 6 shows TEM image of the extracted A0.3M10S10T3 nanocomposite which is exfoliated as revealed by XRD. The clay is well exfoliated in the polymer matrix and large silicate particles are absent.

3.5. Thermal characterization of nanocomposites

The TGA analysis of unextracted nanocomposites is shown in Fig. 7. As the clay content increases, the onset temperature of thermal decomposition at 20% weight loss moves slightly toward a higher temperature. The exfoliated nanocomposite with 3 wt% of silicate shows 7 °C increase in decomposition temperature at 20% weight loss. This may result from thermal barrier property of clay plate.

3.6. DMA properties of nanocomposites

Fig. 8 shows the trend of storage modulus, E', as a function of the temperature for unextracted nanocomposites. The nanocomposite have a higher dynamic modulus than the neat copolymer. The storage modulus of nanocomposite increases with the amount of silicate. A0.3M10S10T3 nanocomposite shows up to 30% increment in dynamic modulus relative to the neat copolymer at 40 °C. Such large increment is due to high stiffness of individual sheet of MMT.

Fig. 9 shows tan δ of the unextracted A0.3M10S10T nanocomposite series. The glass transition temperatures (T_g) were determined from center of peaks in the tan δ curves. A0.3M10S10T nanocomposites below 3 wt% of clay has almost the same glass transition temperature as the neat copolymer. A0.3M10S10T5 shows a little decrease in glass transition temperature. We think the intercalated morphology has some influence on the glass transition temperature.

3.7. Rheological properties nanocomposites

Nanocomposite materials usually show solid-like or long time relaxation fluid behavior. So, one has to control the prior deformation history of the nanocomposite carefully. For the linear viscoelastic measurements dynamic test was firstly performed for 1 h (at frequency = 10 Hz, strain = 0.01%, which is well in the linear dynamic region) at 200 °C.

The effect of clay loading on linear viscoelasticity of

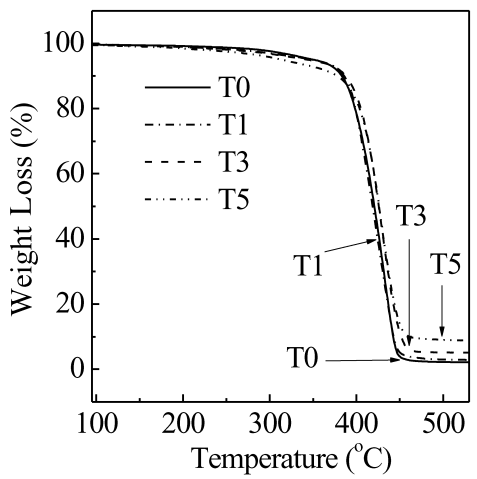

Fig. 7. Thermal gravimetric curves for A0.3M10S10T nanocomposite series and neat copolymer under a nitrogen atmosphere.

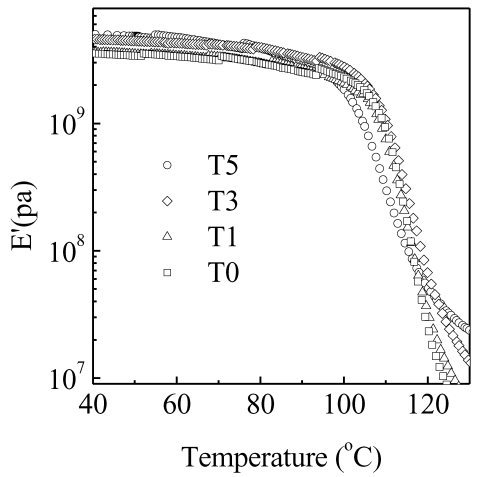

Fig. 8. Dynamic storage modulus of A0.3M10S10T nanocomposite series and neat copolymer as a function of temperature.

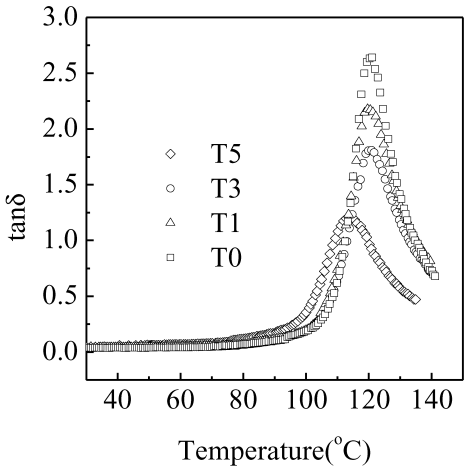

Fig. 9. tan δ of A0.3M10S10T nanocomposite series and neat copolymer as a function of temperature.

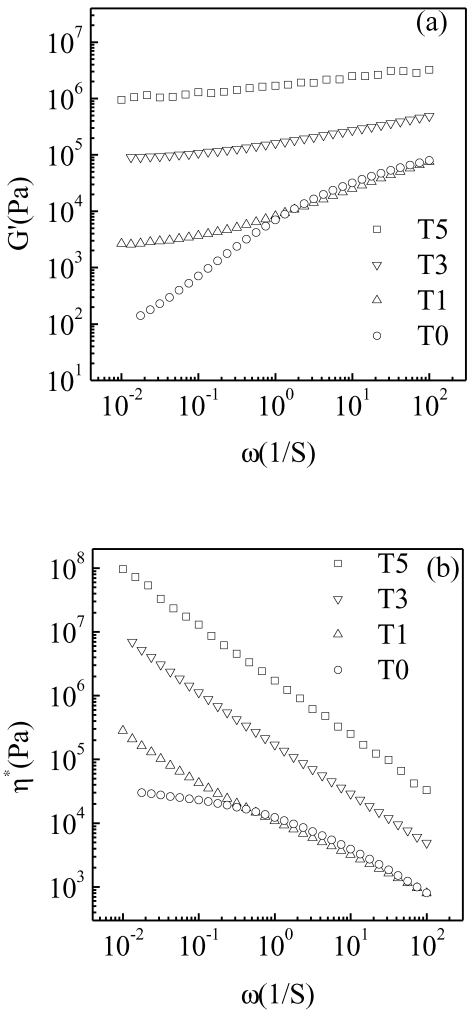

Fig. 10. (a) Storage modulus and (b) complex viscosity of A0.3M10S10T nanocomposite series and neat copolymer as a function of frequency at 200 °C.

P(S-co-MMA)/clay nanocomposites was investigated. The clay concentration was varied from 1.0 to 5.0 wt% (Fig. 10(a)). The nanocomposites show a monotonic increase in storage modulus at all frequencies with increasing silicate content and higher storage moduli than neat copolymer, with the exception of A0.3M10S10T1. A0.3M10S10T1 is regarded to have a higher storage modulus at low frequency because of the effect of clay and to have a lower storage modulus at a high frequency because of the low molecular weight of copolymer than neat copolymer. All nanocomposites exhibit apparent low-frequency plateaus in the linear viscoelastic moduli. This behavior is similar to the response of a viscoelastic solid or a viscoelastic fluid with long characteristic relaxation time. The nanocomposites show a large increase in the complex viscosity with the clay content in, Fig. 10(b). At high clay loadings, they do not show a low-frequency plateau complex viscosity but significant shear thinning behavior. They may have yield stress.

4. Conclusions

A method was described for synthesis of P(S-co-MMA)/Na-MMT nanocomposites through an emulsion polymerization with reactive surfactant AMPS. The synthesis was carried out first by mixing AMPS acid, comonomer with pristine Na-MMT dispersed in water and then by adding comonomer subsequently. The nanocomposite were exfoliated during polymerization. The exfoliated structure of an extracted nanocomposite was further confirmed by TEM.

From XRD patterns of clay dispersion, AMPS widens clay layers and accelerates the insertion of comonomers into clay. For the case of A0.3M10S10T5, MMA occupies a lager portion than styrene in the molecules tethered on clay layers even though the feed ratio of MMA to styrene is the same, because polar MMA has stronger interaction with clay layers.

The onset temperature of thermal decomposition shift toward a higher temperature at 20 wt% loss in TGA as the clay content increases. The dynamic moduli of nanocomposites increase with increasing clay loading. The nanocomposite with 3 wt% of clay shows up to 30% increment in storage modulus relative to neat copolymer. Dynamic storage modulus and complex viscosity increase as the clay content increases. At low frequency all prepared nanocomposites exhibit apparent low-frequency plateaus in the linear storage modulus. Complex viscosity show shear-thinning behavior as the clay content increases.

Acknowledgements

Authors would like to acknowledge financial support from KOSEF (Korea Science and Engineering Foundation)

and CAFPoly (Center for Advanced Functional Polymers). This work was also partially supported by the Brain Korea 21 Program.

References

[1] Pinnavaia TJ, Lan T, Wang Z, Shi H, Kaviratna PD. ACS Symp Ser 1996;622:250.
[2] Lan T, Pinnavais TJ. Chem Mater 1994;6:2216.
[3] Shi H, Lan T, Pinnavais TJ. Chem Mater 1996;8:1584.
[4] Wang Z, Pinnavaia TJ. Chem Mater 1998;10:1820.
[5] Okada A, Usuki A. Mater Sci Engng 1995;C3:109.
[6] Messersmith P, Giannelis EP. Chem Mater 1994;6:1719.
[7] Messersmith PB, Giannelis EP. J Polym Sci, Polym Chem 1995;33: 1047.
[8] Yano K, Usuki A, Okada A, Kurauchi T, Kamigaito O. J Polym Sci, Polym Chem 1993;31:2493.
[9] Gilman JW, Jackson CL, Morgan AB, Harris Jr R, Manias E, Giannelis EP, Wuthenow M, Hilton D, Philips SH. Chem Mater 2000; 12:1866.
[10] Choi MH, Chung IJ, Lee JD. Chem Mater 2000;12:2977.
[11] Byun HY, Choi MH, Chung IJ. Chem Mater 2001;13:4221.
[12] Wang KH, Xu M, Choi YS, Chung IJ. Polym Bull 2001;46:499.
[13] Choi YS, Wang KH, Xu M, Chung IJ. Chem Mater 2002;14:2936.
[14] Wang KH, Choi MH, Koo CM, Xu M, Chung IJ, Jang MC, Choi SW, Song HH. J Polym Sci, Part B: Polym Phys 2002;40:1454.
[15] Usuki A, Kawasumi M, Kojima Y, Okada A, Kurauchi T, Kamigaito O. J Mater Res 1993;8:1174.
[16] Usuki A, Kojima Y, Kawasumi M, Okada A, Fukushima Y, Kurauchi T, Kamigaito O. J Mater Res 1993;8:1180.
[17] Kojima Y, Usuki A, Kawasumi M, Okada A, Fukushima Y, Kurauchi T, Kamigaito O. J Mater Res 1993;8:1185.
[18] Pinnavaia TJ. Science 1983;220:365.
[19] Murray HH. Appl Clay Sci 2000;17:207.
[20] Vaia RA, Teukosky RK, Giannelis EP. Chem Mater 1994;6:1017.
[21] Krishnamoorti R, Vaia RA, Giannelis EP. Chem Mater 1996;8:1728.
[22] Krishnamoorti R, Giannelis EP. Macromolecules 1997;30:4097.
[23] Limary R, Swinnea S, Green PF. Macromolecules 2000;33:5227.
[24] Ren J, Silva AS, Krishnamoorti R. Macromolecules 2000;33:3739.
[25] Lyatskaya Y, Balazs AC. Macromolecules 1998;31:6676.
[26] Balazs AC, Singh C, Zhulina E. Macromolecules 1998;31:8370.
[27] Zhulina E, Singh C, Balazs AC. Langmuir 1999;15:3935.
[28] Balazs AC, Singh C, Zhulina E, Lyatskaya Y. Acc Chem Res 1999; 32:651.
[29] Ginzburg VV, Balazs AC. Adv Mater 2000;12:1805.
[30] Akelah A, Salahuddin N, Hiltner A, Baer E, Moet A. Nanostruct Mater 1994;4:965.
[31] Akelah A, Moet A. J Mater Sci 1996;31:3589.
[32] Moet A, Akelah A. Mater Lett 1993;18:97.
[33] Giannelis EP. Adv Mater 1996;8:29.
[34] Hoffmann B, Dietrich C, Thomann R, Friedrich C, Mülhaupt R. Macromol Rapid Commun 2000;21:57.
[35] Fu X, Qutubuddin S. Mater Lett 2000;42:12.
[36] Fu X, Qutubuddin S. Polymer 2001;42:807.
[37] Weimer MW, Chen H, Giannelis EP, Sogah DY. J Am Chem Soc 1999;121:1615.
[38] Vaia R, Ishii H, Giannelis E. Chem Mater 1993;5:1694.
[39] Sikka M, Cerini LN, Ghosh SS, Winey KI. J Polym Sci, Part B: Polym Phys 1996;34:1443.
[40] Kelly P, Akelah A, Qutubuddin S, Moet A. J Mater Sci 1994;29:2274.
[41] Vaia RA, Jandt KD, Kramer EJ, Giannelis EP. Macromolecules 1995; 28:8080.
[42] Friedlander HZ, Grink CR. J Polym Sci, Polym Lett 1964;2:475.
[43] Kato C, Kuroda K, Takahara H. Clays Clay Miner 1981;29:294.
[44] Chen G, Ma Z. Scripta Mater 2001;44:125.
[45] Blumstein A. J Polym Sci, Polym Chem 1965;3:2653.
[46] Blumstein A. J Polym Sci, Polym Chem 1965;3:2665.
[47] Bhattacharya J, Chakraborti SK, Talapatra S. J Polym Sci, Polym Chem 1989;27:3977.
[48] Chen G, Chen X, Lin Z, Ye W, Yao K. J Mater Sci, Lett 1999;18: 1761.
[49] Okamoto M, Morita S, Taguchi H, Kim YH, Kotaka T, Tateyama H. Polymer 2000;41:3887.
[50] Lee DC, Lee WJ. J Appl Polym Sci 1996;61:1117.
[51] Biasci A, Aglietto M, Ruggeri G, Ciardelli F. Polymer 1994;35:3296.
[52] Sato H, Taguchi H, Sato N, Okamoto M, Kotaka T. Polym Prep Jpn 1997;46:2719.
[53] Huang X, Brittain WJ. Macromolecules 2001;34:3255.
[54] Zeng C, James L. Lee. Macromolecules 2001;34:4098.
[55] Choi YS, Choi MH, Wang KH, Kim SO, Kim YK, Chung IJ. Macromolecules 2001;34:8978.
[56] Seki M, Morishima Y, Kamachi M. Macromolecules 1992;25:6540.
[57] Morishima Y, Nomura S, Ikeda T, Seki M, Kamachi M. Macromolecules 1995;28:2874.
[58] Aota H, Akaki SI, Morishima Y, Kamachi M. Macromolecules 1997; 30:4090.
[59] Heffner SA, Bovey FA, Verge LA, Mirau PA, Tonelli AE. Macromolecules 1986;19:1628.